Indian Journal of Pure & Applied Physics
Vol. 55, February 2017, pp. 122-128

Preparation of iodine and silver coated thin film on poly(methylmethacrylate) substrate and examination of antifungal, antibacterial and mechanistic properties

S E Kariper[a], C Hepokur[b], İ A Kariper[c]*, İ Üstündağ[d] & D Ceylan[e]

[a]Chemistry Department, Science Faculty, Cumhuriyet University, Sivas, Turkey

[b]Pharmacology Faculty, Cumhuriyet University, Sivas, Turkey

[c]Education Faculty, Erciyes University, Kayseri, Turkey

[d]Physics Department, Faculty of Arts & Science, Dumlupınar University, Kütahya, Turkey

[e]Science Institution, Erciyes University, Kayseri, Turkey

Received 14 June 2016; revised 6 September 2016; accepted 4 November 2016

In this study, iodine (I_2) and silver (Ag) have been deposited on polymer substrate, namely poly(methylmethacrylate), via chemical bath deposition (CBD). For the sake of simplicity, uncoated poly(methylmethacrylate), iodine coated poly(methylmethacrylate) thin film and silver coated iodized thin film on poly(methylmethacrylate) have been denoted as PMM, I_2-PMM and Ag-I_2-PMM. Capacitance of the film has been measured with a LCR meter, whereas surface tensions were measured by a tensiometer. Transmittance, reflectance and absorption properties of thin films have been investigated via an UV-vis spectrometer. Elemental composition of uncoated PMM and thin films has been discovered by means of energy dispersive X-ray (EDX). Elemental composition of uncoated PMM has been determined as 64% C and 36% O, whereas Ag-I_2-PMM contained 28% iodine and 23% silver. X-ray photoelectron spectroscopy (XPS) has been employed to characterize the surface structure of I_2-PMM and Ag-I_2-PMM. In addition, antimicrobial properties of the silver coated material have been examined.

Keywords: Silver coating, Iodine coating, Thin film characterization, Antibacterial-antifungal properties

1 Introduction

Iodine coated materials show anti-microbial and anti-infective properties. According to some studies, source of HIV and hepatitis viruses may be some clinic and laboratory tools, and patient care items that came in contact with blood or humoral fluids. They have the potential of infecting patients, health personnel and the humans if released in the environment. These infections are becoming a serious health menace because of the drastically rising number of the people infected by these viruses. These problems direct the researches to look for the ways of coating hospital and laboratory equipment with iodine[1,2]. Kristinsson *et al.*[3] solved this problem by coating iodine on polyvinylpyrrolidone, whereas Domb and Shikani[1] used polyvinyl- pyrrolidone, methyl methacrylate, vinyl pyrrolidone and polyurethane.

Silver coated materials are not only used for their anti-microbial or antibacterial properties, they are also used in high reflectance applications in the visible and infrared regions. High reflectance of silver coating materials is very useful for material science, whereas their anti-microbial or antibacterial properties are useful for medical applications. Kobayashi *et al.*[4] coated silver nano particles via Stöber method and worked on surface modification. Knetsch and Koole[5] have studied silver nanoparticles/polymer composite material. These nanomaterials prevent medical device related infections. Silver nanoparticles are also used in solar cell researches. Choi *et al.*[6] has examined polymer based solar cells using the plasmonic effect of multi positional silica covered AgNPs. They reported that the location of the nanoparticles is very important for increasing light absorption and scattering by means of enhanced electric field distribution[6].

All these studies show that some properties of iodine or silver coated materials are changing and they are very useful materials with their anti-microbial, antibacterial, anti-infective (medical applications), high reflectance, plasmonic effect (physical properties) properties.

There are various modification methods in the literature. Some of these methods are chemical (electrochemical[7,8], chemical vapor deposition[9], self-assemble monolayers[10] and CBD[11,12] techniques) and some of them are physical (physical vapor

*Corresponding author (E-mail: akariper@gmail.com)

deposition[13], e-beam lithography[14], sputtering[15], Langmuir-Blodget (LB)[16], layer by layer (LBL)[17] and plasma[18] techniques). CBD is a very simple, low-cost and powerful technique for various surface modifications. Castillo *et al.*[19] studied the effect of using hydrazine and ammonia–hydrazine as alternative complexing agents for producing PbS thin films via CBD technique. Lee and co-workers[20] grew vertical ZnO nanorods on seeded Si platform using CBD technique combined with radio frequency (RF) sputtering. Iwashitaa and Ando[21] covered ZnS by using CBD method. They characterized the modified layer through XRD, SEM, EDX and light transmission.

In this study, iodine and silver were attached to PMM surface via chemical bath deposition. Each thin film was characterized by LCR meter, tensiometer, and spectroscopic methods such as UV-visible, EDX and XPS. Also, antibacterial and antifungal properties of Ag-I_2-PMM were examined.

2 Experimental

2.1 Preparation of films

All chemicals were procured from Merck, and Sigma-Aldrich and they were used without further purification. The substrates were cleaned in ultrapure water (UPW) and ethanol. 0.001 mole silver nitrate and iodine (I_2) were solved in 100 mL ethanol, in different beakers. PMM substrates were dipped into these beakers at room temperature. These chemical baths were kept at 60 °C in the oven, for 2 h. The obtained thin films were cleaned in UPW and dried prior to examinations. Some properties of these films were examined as explained in measurement and materials part. Antibacterial and antifungal properties of silver coated films were examined and explained at the end of result and discussion section.

2.2 Measurement and materials

The capacitance measurements, which is the measurement made under 10 V constant voltages by scanning between 20 and 2 MHz, were performed by an Aligent LCR meter at room temperature. The electrodes were prepared with silver paste, their surface areas were 100 mm^2 and the distance between them was 4 mm. PMM coating process and photographs are shown in Fig. 1(a) and 1(b). XPS measurements of I_2-PMM and Ag-I_2-PMM surfaces were carried out with a PHI 5000 Versa Probe (ϕ ULVAC-PHI, Inc., Japan/USA) model X-ray photoelectron spectrometer (under monochromatized Al-Kα radiation (1486.6 eV) as an X-ray anode operated at 50 W with the pressure inside the analyzer was maintained at 10^{-7} Pa). The crystalline structure of Ag-I_2-PMM film was confirmed by XRD (Rikagu RadB model, λ=1.5406 Å) with a CuKα_1 radiation source over the range 10° <2θ<90° at a speed of 3° min^{-1} with a step size of 0.02°. The surface properties of all films were characterized by using computer controlled digital SEM (EVO40-LEO). Chemical composition analysis of the nano films were performed using an EDX spectrometer attached to SEM. Surface tensions were measured with a KSV CAM200 tensiometer (Finland), at room temperature, in airflow controlled conditions. Contact angle measurements were performed via concentrated

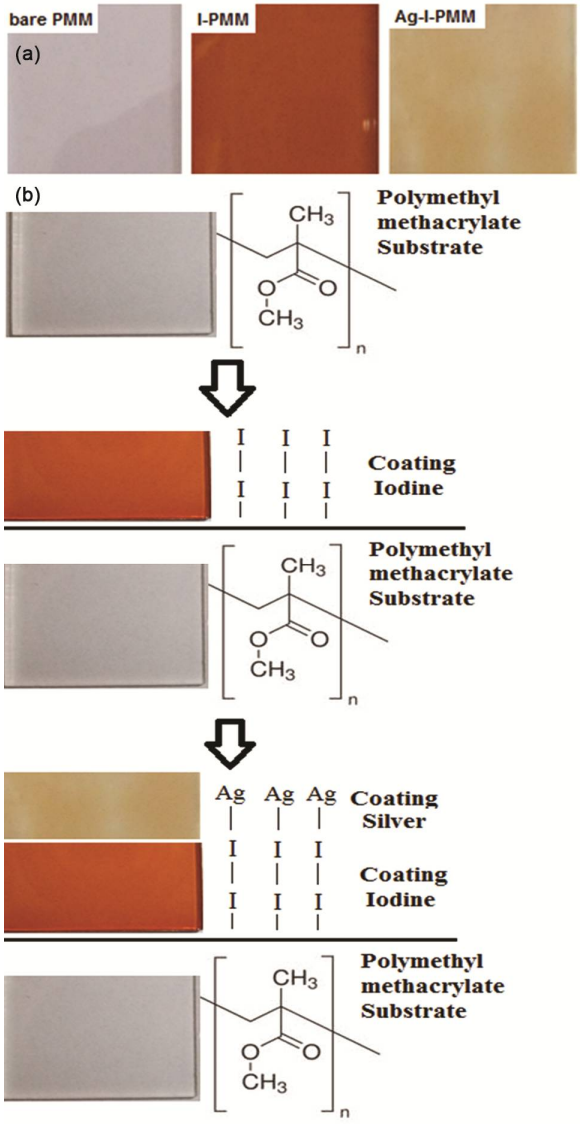

Fig. 1 – (a) Photographs of bare PMM, iodine coated PMM (I-PMM) and silver deposited iodine coated PMM (Ag-I-PMM) and (b) coating process schemes of iodine and silver covered films

glycerin, iodometane, deionized water and ethylene glycol. The surface tension of the liquids was measured with pendant drop method and their purity was checked prior to usage.

2.3 Antibacterial efficiency of the modified surfaces

Antibacterial activity of the modified surface was examined against facultative gram-negative *Escherichia coli* (ATCC 25922). The bacteria were cultured in the Luria Broth (LB) medium at 37 °C for 24 h, at 200 rpm. The cultured *E-coli* were diluted to reach the concentration of bacteria corresponding to 1 of MacFarland scale (10^8 colony forming units per milliliter CFU/mL). Samples of uncoated substrate and modified surfaces were put on a tray and incubated with calibrated fungal suspension of *E-coli* at 37 °C for 24 h.

2.4 Antifungal efficiency of the modified surfaces

Antifungal efficiency of the modified surfaces was checked using diploid fungus. Candida Albicans (ATCC 90028) was prepared using sterile YEPD (1% yeast extract, 2% peptone, 2% dextrose) solution in 20% glycerol at 0,5 McFarland turbidity. The treated cells were diluted to 6.5×10^6 colony forming units (CFU/mL) with sterilized UPW. 1 mL portioned suspensions were stored at –80 °C. Growth suspension (65 g of sabouraud dextrose agar was dissolved in 1 L of UPW and autoclaved for 1.5 h) was prepared. The solution was cooled, poured and dispersed into petri dishes. The precipitate was stored for a night in a fridge before application. Then, C. albicans were incubated on Petri plates using Sabouraud, Dextrose-Agar growth media, at 37 °C for 24 h. The treated fungi were aerobically grown for 48 h, at 25 °C, in YEPD suspension. Uncoated PMM and modified PMMs were placed on a tray and incubated with a calibrated fungal standard solution of C. Albicans and kept at 37 °C for 24 h.

3 Results and Discussion

AgI and AgCl peaks can be observed at $10<2\theta<90$ diffraction angle in the XRD spectrum. These diffraction patterns had cubic (AgI) and (AgCl) structures and their preferential orientation in (220), (100), (102) and (311) plane are observed at peak 1, 2, 3 and 4, respectively. These results are displayed in Fig. 2 and Table 1. The peaks were indexed by XRD-EVA program, however some AgI peaks that were indexed by the program were not taken into consideration in Fig. 2 (because of intensity of these peaks falls to 10%). These results may help us to better understand the structure and composition of the coated material. XRD pattern shows that some AgCl peaks can be clearly observed in Fig. 2; in addition no chlorine contamination was detected in Fig. 3. Since the percentage of chlorine is lower than the other atoms, chlorine peaks could not be observed in EDX analysis (approximately 1 or 2%). Elemental compositions of PMM and modified surfaces were characterized by EDX technique. The results of EDX analysis are given in Fig. 3. Chemical composition of PMM was calculated as 64% C and 36 % O, whereas the composition of I_2-PMM was determined as 67% C, 29% O and 4% I. EDX analysis results of Ag-I_2-PMM was found to be 36% C, 13% O, 28% I and 23% Ag. According to EDX analysis results, iodine and silver were grafted on PMM surface. Figure 3 shows SEM images and photos of the films and PMM, which shows that uncoated PMM has a simple and smooth surface. Coating iodine on PMM surface was resulted with a swollen and rough surface, whereas coating Ag on I_2-PMM caused the formation of grains. The amorphous surface of PMM and I_2-PMM were clearly observed. Crystalline grains of Ag on the I-PMM surface was observed in its' SEM image. These SEM images were taken at 200 nm, so, the grain size of Ag on the coating film can be estimated to be around 50 nm. Besides reflectance (*R*), transmittance (*T*) and absorbance (*A*) values of

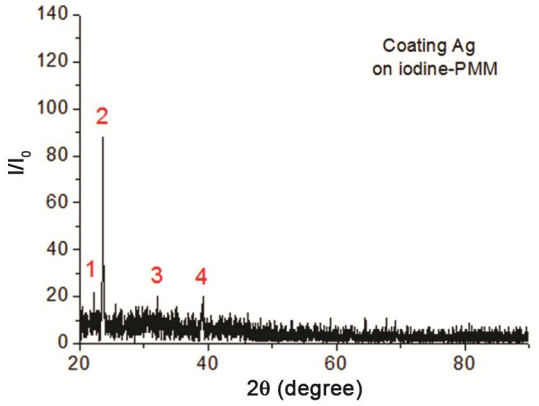

Fig. 2 – XRD pattern of coating silver on iodine-PMM

Table 1 – XRD data of the coating silver on iodine-PMM

Peak number	Compound	*hkl*	2θ (observed)	2θ (calculated)	Structure
1	AgI	220	22.238	22.360	Cubic
2	AgI	100	23.614	23.694	
3	AgC1	102	32.208	31.566	
4	AgI	311	39.308	39.175	

PMM, I_2-PMM and Ag-I_2-PMM can be calculated with the equality below:

$$T = (1-R)^2 e^{-A} \quad \ldots (2)$$

Transmittance and absorbance measurements were performed at room temperature, in the range of 300-1100 nm by UV-Vis spectrophotometer. Transmission and reflectance (%) of PMM, I_2-PMM and Ag-I_2-PMM are presented in Fig. 4. The highest transmittance was observed on PMM while the lowest transmittance was observed on Ag-I_2-PMM. The transmittance of I_2-PMM tended to drop under 700 nm wavelength. On the other hand, the highest reflectance was observed on Ag-I_2-PMM while the lowest reflectance was observed on PMM. The iodine reflectance curve showed an oscillator move. The absorbance curves of PMM, I_2-PMM and Ag-I_2-PMM are shown in Fig. 5. Absorbance curves behaved as reflectance curves. Also, iodine absorption of the nano film was observed between 260-280 nm, 323 nm and 407 nm. Wei and co-workers have observed two absorption bands at 193 and 226 nm for I^- form[22]. In the paper, I_3^- absorption bands appeared at 288 and 350 nm in the aqua solutions and mixed KI solutions, respectively. Since both of I^- and I_3^- form of absorption was observed, we used I- symbols in the graphics. XPS survey spectra of I_2-PMM and Ag-I_2-PMM surfaces are given in Fig. 6(a) and this shows that I_{3d} binding energy[23-24] of I_2-PMM was found to be around of 620 eV. In Fig. 6(b), I_{3d} and Ag_{3d} binding energies[25] of Ag-I_2-PMM were determined around 620 eV and 375 eV, respectively. The resistivity of PMM, I_2-PMM and Ag-I_2-PMM were measured by four-point measurements using the following relations:

$$\rho = 2\pi s \frac{V}{I} (t >> s) \quad \ldots (2)$$

$$\rho = \frac{\Pi t}{\mathrm{In}2} \frac{V}{I} (t << s) \quad \ldots (3)$$

Here, t is thickness of thin film, V is the potential value, I is the current, and s is the distance between the probes. Regarding Eq. (2), the distance between

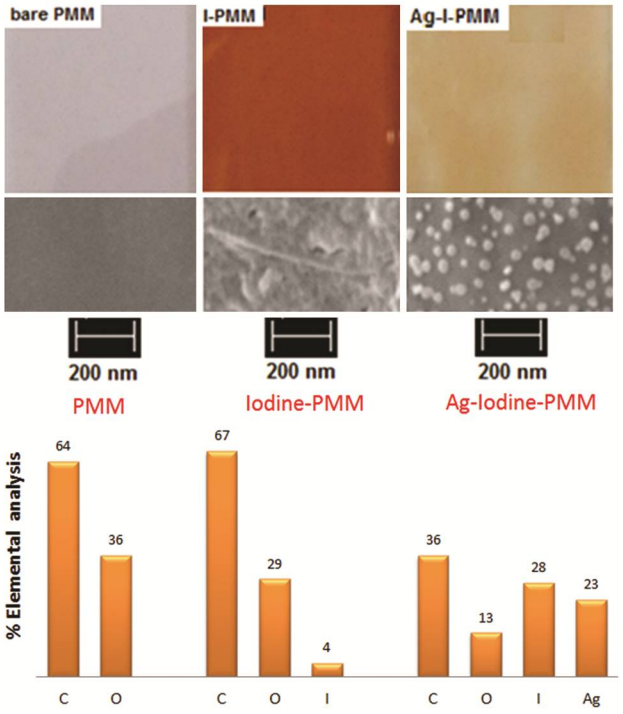

Fig. 3 – EDX analysis results and SEM images-photos of bare poly(methylmethacrylate) substrate, iodine coated PMM surface and silver attached iodized thin film on PMM

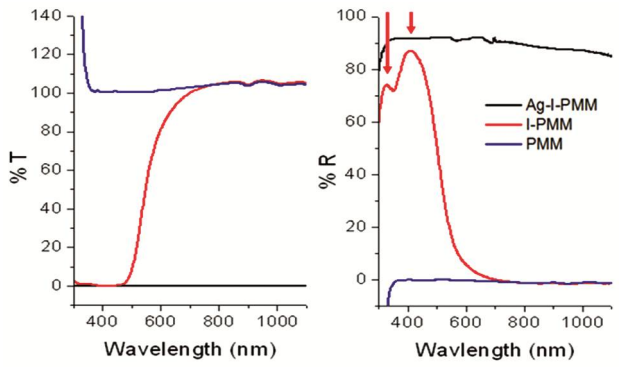

Fig. 4 – Change of % *T* and % *R* with wavelength of PMM, iodine-PMM and silver-iodine-PMM

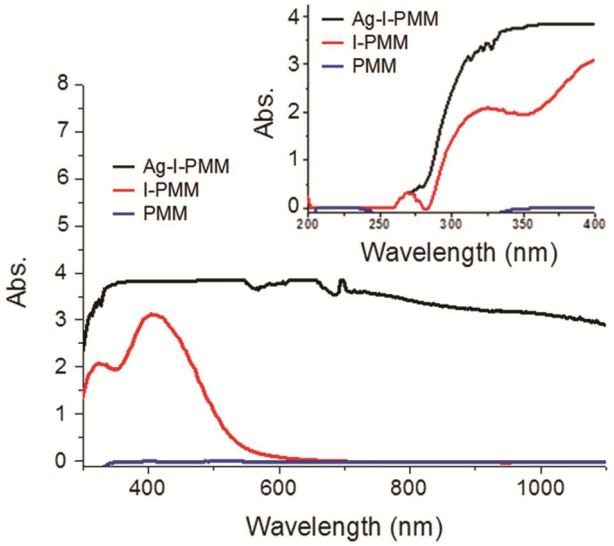

Fig. 5 – Change of absorbance with wavelength of bare PMM, iodine-PMM and silver-iodine-PMM

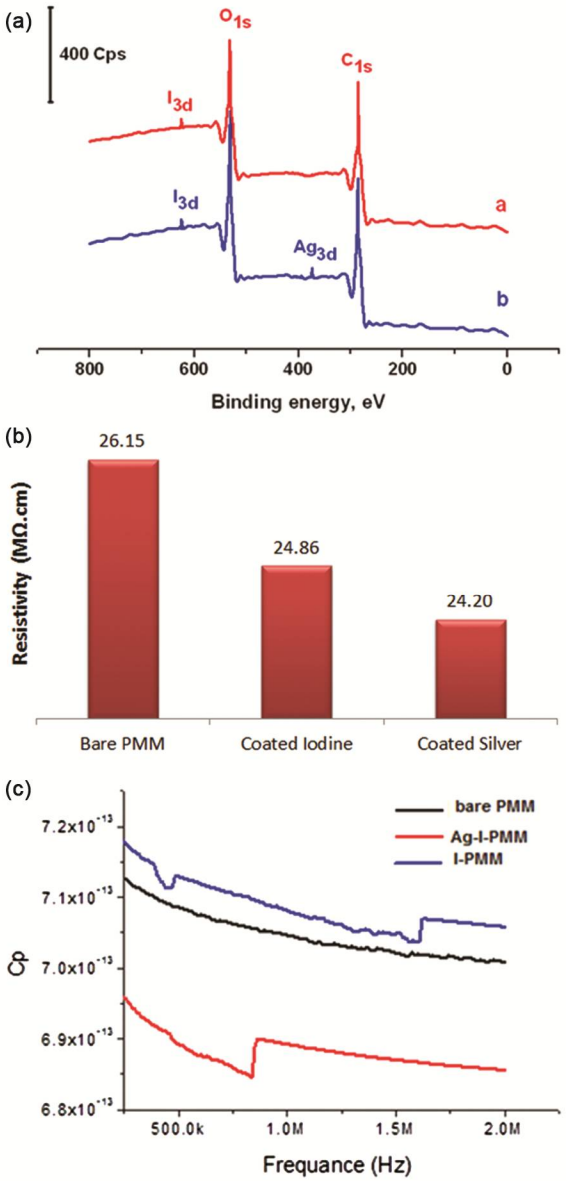

Fig. 6 – XPS Survey spectra (a) Resistivity and (b) the capacitance of iodine coated PMM surface and silver attached iodized thin film on PMM

the probes was taken in millimeter whereas film thickness was in nanometer during the measurements. Here, we didn't use Eq. (2), because silver and iodine deposited PMM would behave as bulk material. At this point, we want to examine the effect of the coating on the resistance of the material. In addition, we didn't measure the thickness of the iodine and silver films. The resistivity of PMM, I_2-PMM and Ag-I_2-PMM are presented in Fig. 6(b).

Figure 6(c) presents the capacitance values of PMM, I_2-PMM and Ag-I_2-PMM. We expected to decrease the resistivity of PMM by coating it with iodine and silver. A small decrease of resistance can be seen in Fig. 6(b). This is because the gap between the grains was increased by coating PMM with iodine and silver. This can be clearly observed in SEM images. The researchers found the resistivity of PMM as 2.58×10^5 Ω.cm through four-point probe[26]. At this point, we are not concerned about the numeric value of resistivity. We are interested in the impact of coating PMM substrate with iodine and then silver on its resistance. These values are also an indicator showing the variation of capacitance values. The capacitance of I_2-PMM, which goes up to 0.72 pF (Fig. 6(c)), is the highest capacitance, whereas the capacitance of Ag-I_2-PMM falls up to 0.6 pF. There are breaks in the capacitance curve of I_2-PMM and Ag-I_2-PMM, due to sudden discharge of silver and iodine. The charges deposited in the PMM substrate by the carbonyl groups are discharged to the iodine and silver coating. Since silver and iodine have different conductivity and dielectric properties, we observed each coating on different frequencies. In addition, resistivity decreased by coating PMM with iodine and silver. This capacitance decrease had been observed before in the literature[27-28]. Zisman found that cosθ is a function γ_l:

$$\cos\theta = a - b\gamma_t = 1\beta(\gamma_t - \gamma_{cr}) \quad \ldots (4)$$

$$E_b \text{ and } E_f\,(\%) = [(A–B)]\times100\% \quad \ldots (5)$$

γ_{cr} is critical surface tension of a solid and it is a characteristic feature of any given solid. Any liquid with $\gamma_l<\gamma_{cr}$ will wet to the surface. The measured critical surface tension[29] is very close to the one of solid surface, thus this method can be applied to thin films as well, $\gamma_s\sim\gamma_{cr}$. The critical surface tension of the material can be found using cosθ value of the curve obtained from surface tension graphics of the liquids, then this value can be computed by simulation, from $y = Ax + B$ curve. x value for y=1 can be calculated from this equitation. Figure 7(a), (b) and (c) shows the surface tensions and contact angle of PMM, I_2-PMM and Ag-I_2-PMM. A linear equation, similar to 7(a), (b) and (c) was developed. Accordingly, surface tensions of PMM, I_2-PMM and Ag-I_2-PMM were found to be 30.27, 28.77 and 32.65 mN/m, respectively. These results indicate that coating Ag on PMM surface increased critical surface tension. In SEM images, we have observed that Ag-I_2-PMM has rougher surface than I_2-PMM.

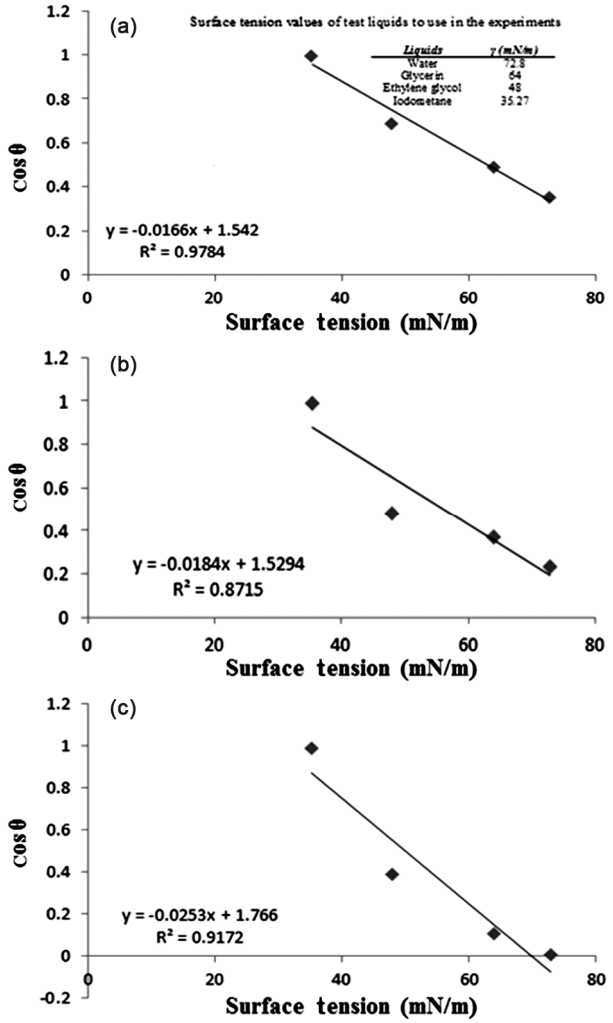

Fig. 7 – (a) The surface tensions and contact angles of bare poly(methylmethacrylate), (b) the surface tensions and contact angles of iodine coated thin films and (c) the surface tensions and contact angles of silver coated thin films on iodine-PMM.

Antibacterial efficiency (E_b) and antifungal efficiency (E_f) were calculated according to the following equation:

$$E_b \text{ and } E_f\,(\%) = [(A–B)/A]\times 100\% \quad \ldots (5)$$

Here, A and B are the number of viable bacteria or fungus observed on the uncoated sample and the number of viable bacteria or fungus observed on the modified samples in the tray (Control=24×10^5, for antibacterial test and Control= 78×10^5, for antifungal test). Figure 8 shows antibacterial and antifungal properties of Ag-I_2-PMM.

Antibacterial efficiency of Ag-I_2-PMM was up to 95% at 48 h, while its antifungal efficiency was up to 95% at 96 h. Even though silver coated films are

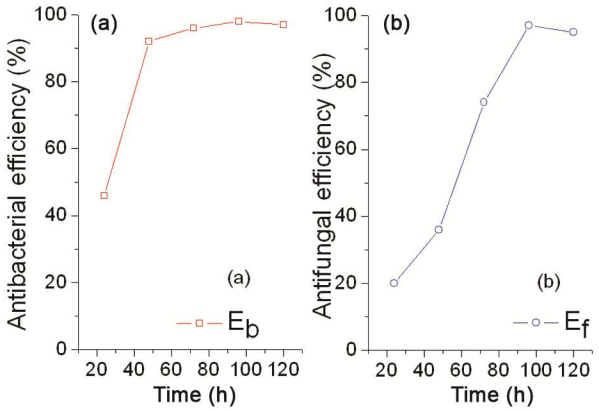

Fig. 8 – (a) Antibacterial and (b) antifungal efficiencies of silver on iodine-PMM

well-known with their antibacterial property in the literature, researchers did not focus on their antifungal properties much. Ghafari-Nazari *et al.* studied antibacterial activity of silver photo deposited nepheline modified thin film. They used to 1.6×10^3 mL^{-1} S aureus and E. coli in their experiment. They calculated[30] that the bacteriostatic activity of SiO_2 against E coli was 30%. Tatar *et al.* produced silver thin films on glass substrate. They observed that antibacterial thin film was effective when the percentage[31] of silver in their films was over 3-5%. Trindade *et al.* attempted to determine antifungal properties of silver thin films. They incubated fungal colonies for four days. Antifungal efficiency[32] of the films with 0.803 mg/g silver and 62 µm thickness was 45%. The films used in this study are more advantageous than the ones mentioned in the literature, because other researchers have used low number of colony, excess silver or thicker films compared to the ones in this study.

4 Conclusions

Chemical bath is a very easy method for the modification of thin films. We have successfully produced iodine coated thin films and Ag coated iodine thin films by using CBD method on PMM. Deposited thin films were characterized via various physical methods such as capacitance and surface tensions measurements. Spectroscopic characterization was performed by using UV-Vis, Spectrometry (transmittance, reflectance and absorption measurement), XPS and EDX techniques. I_{3d} binding XPS spectrum of I_2-PMM and I_{3d}-Ag_{3d} binding XPS spectra of Ag-I_2-PMM were revealed by XPS analysis. The chemical composition of uncoated PMM and modified PMMs were characterized through EDX measurements. Elemental quantity of the PMM was determined as

64% C and 36% O. 28% iodine and 23% silver were detected in Ag-I_2-PMM. Also, antibacterial and antifungal properties of Ag-I_2-PMM were examined. The antibacterial efficiency after 48 h and the antifungal efficiency after 96 h were observed to be up to 95 %.

References

1 Domb A J & Shikani A H, US5695458, 28 Jan 1999.
2 Davydov A B, Belyh S I & Kravets V V, *Biomed Eng*, 46 (2013) 237.
3 Kristinsson K G, Jansen B, Treitz U, Schumacher-Perdreau F, Peters G & Pulverer G, *J Biomater Appl*, 5 (1991) 173.
4 Kobayashi Y, Katakami H, Mine E, Nagao D, Konno M & Liz-Marzán L M, *J Colloid Inter Sci*, 283 (2005) 392.
5 Knetsch M L W & Koole L H, *Polymers*, 3 (2011) 340.
6 Choi H, Lee J P, Ko S J, Jung J W, Park H, Yoo S, Park O, Jeong J R, Park S & Kim J Y, *Nano Lett*, 13 (2013) 2204.
7 Liu Y, Gokcen D, Bertocci U & Moffat T P, *Science*, 338 (2012) 1327.
8 Hong Y K, Yu H, Lee T G, Lee N, Bahng J H, Song N W, Chegal W, Shon H K & Koo J Y, *Chem Phys*, 428 (2014) 105.
9 Tallaire A, Achard J, Boussadi A, Brinza O, Gicquel A, Kupriyanov I N, Palyanov Y N, Sakr G & Barjon J, *Diamond Relat Mater*, 41 (2014) 34.
10 Göhler B, Hamelbeck V, Markus T Z, Kettner M, Hanne G F, Vager Z, Naaman R & Zacharias H, *Science*, 331 (2011) 894.
11 Narhe R D, González-Viñas W & Beysens D A, *Appl Surf Sci*, 256 (2010) 4930.
12 Gao C, Shen H & Sun L, *Appl Surf Sci*, 257 (2011) 6750.
13 Avelar-Batista Wilson J C, Banfield S, Eichler J, Leyland A, Matthews A & Housden J, *Thin Solid Films*, 520 (2012) 2922.
14 Jiang W, Hu S, Xie C, Zhu X, Zhao L, Xie W, Wang J & Dong X, *Microelectron Eng*, 88 (2011) 3178.
15 Insepov Z, Yamada I & Sosnowski M, *Mater Chem Phys*, 54 (1998) 234.
16 Zhang Q, Huang D & Liu Y, *Synthetic Met*, 137 (2004) 989.
17 Deshmukh P K, Ramani K P, Singh S S, Tekade A R, Chatap V K, Patil G B & Bari, S B, *J Control Release*, 166 (2013) 294.
18 Chen H, Li J, Shao D, Ren X & Wang X, *Chem Eng J*, 210 (2012) 475.
19 Castillo A C, Ambrosio Lázaro R C, Jimenez-Pérez A, Martínez Pérez C A, De la Cruz Terrazas E C & Quevedo-López M A, *Mater Lett*, 121 (2014) 19.
20 Lee T H, Ryu H & Lee W J, *J Alloy Compd*, 597 (2014) 85.
21 Iwashitaa T & Ando S, *Thin Solid Films*, 520 (2012) 7076.
22 Wei Y J, Liu C G & Mo L P, *Spectro Spect Anal*, 25 (2005) 86.
23 Dowben P A, Grunze M & Tomanek D, *Physica Scripta*, 4 (1983) 106.
24 Lei J, Rudenja S, Magtoto N & Kelber J A, *Thin Solid Films*, 497 (2006) 121.
25 Schlatterbeck D, Parschau M & Christmann K, *Surf Sci*, 418 (1998) 240.
26 Kariper İ A & Ozpozan T, *J Nanomater*, 2013 (2013) 9.
27 Ramu C H, Naidu Y R V & Sharma A K, *Ferroelectrics*, 159 (1994) 275.
28 Kiran S, Santhosh N K & Naveen S K, *AIP Conf Proc*, 1536 (2013) 511.
29 Fox H W & Zisman W A, *J Colloid Sci*, 7 (1952) 109.
30 Ghafari-Nazari A, Moztarzadeh F, Rabiee S M, Rajabloo T, Mozafari M & Tayebi L, *Ceram Int*, 38 (2012) 5445.
31 Tatar P, Kiraz N, Asilturk M, Sayılkan F, Sayılkan H & Arpac E, *J Inorg Organomet P Mater*, 17 (2007) 525.
32 Pinto R J B, Almeida A, Fernandes S C M, Freire C S R, Silvestre A J D, Neto C P & Trindade T, *Colloid Surf B: Biointerfaces*, 103 (2013) 143.